Proc. Symposium on Personal Wireless Comm., **Blacksburg, VA, June 1997**

Integrated I-Q Demodulation, Matched Filtering, and Symbol-Rate Sampling Using Minimum-Rate IF Sampling

Dan P. Scholnik and Jeffrey O. Coleman

Department of Electrical Engineering
Michigan Technological University
Houghton, MI 49931-1295
scholnik@wizard.nrl.navy.mil jeffc@mtu.edu

Abstract

The samples of the complex modulation envelope I+jQ typically required in coherent communication are sometimes obtained without cumbersome analog hardware by bandpass sampling the IF signal. Most published systems offer limited design flexibility, especially in the design of the digital filtering that ultimately determines system performance. We present here a generalization of such systems (derived from the analog modulator that it replaces) along with a mathematically equivalent system that simplifies analysis. By combining most design choices into a single equivalent filter response, the intuition of the filter designer can go far towards suggesting suitable approaches for individual applications, while the large number of available digital-filter design tools makes custom design practical. Two examples demonstrate a simple approach to design using available tools.

1 Introduction

A common procedure in communication and radar systems (among others) is the demodulation of passband signals to baseband. Traditionally, a pair of analog mixers driven by quadrature carriers is used to demodulate the I and Q components of the signal in two parallel arms. Identical analog lowpass filters then follow the mixers, with their output often sampled for digital processing. The analog hardware in this classic quadrature demodulator presents a stiff challenge: it requires carriers in perfect quadrature and responses must be matched between the I and Q arms. Mixer nonlinearities, component drift, mismatched filter responses, and quadrature carrier mismatches are all potential sources of error. The rise in performance in digital-signal-processing hardware and A/D converters offers an alternative: directly sample the bandpass signal, and use digital processing to recover the complex modulation envelope. By using a single A/D to sample the IF signal directly, mismatch between signal paths is eliminated, as is the need for quadrature carriers. Thereafter all processing enjoys the precision of the digital domain.

The idea of directly sampling a bandpass signal for demodulation is not new. In the 1950's Kohlenberg [1] and Linden [2] described sampling theorems for first and second order sampling and reconstruction of bandpass waveforms. More recently, Coulson [3] extended these sampling theorems and implemented them digitally by sampling the interpolating functions. The first attempts to implement these ideas appear to be separate efforts by Waters and Jarrett [4] and Rice and Wu [5], published in the same issue in 1982 and describing essentially identical systems. Both describe

systems that replace the I and Q arms of the analog demodulator with two separate sampling and filtering arms. Many papers since have described similar or identical systems: [6–12] is a partial list. In 1984 Rader [13] introduced a different sampling scheme that involved sampling at four times the IF frequency, digitally filtering and decimating by four. Although this can be viewed as a bandpass sampling system, it is also a conventional lowpass sampling system by virtue of sampling at twice the highest frequency of the bandpass input. Rader used IIR filters in his paper; Mitchell [14] extended it to FIR filters, and Ward [15] used a least-mean-square-error statistical model for filter design. Other systems similar to Rader's are described in [16–18]. Pohlig [19], presents a different implementation which appears to be unique in the literature. Each system is potentially limited by specific requirements on key system parameters and filter types (Pohlig [19] hints at some of the generalizations presented here), and only [18] considers spectral shaping as part of the filtering process.

The ability to intuitively and intelligently design such systems requires a model that is simultaneously simple, general, implementable, and that allows a straightforward approach to filter design. As performance of the system inevitably hinges on the latter, the presented model emphasizes an approach in which most design choices are collapsed into a single equivalent filter response.

This paper is presented in three sections. The first section lays out some basic signal-processing system transformations that will be used in the second section, where both an analytical model and two implementations will be derived from the classic analog demodulator. The last section presents some design examples to demonstrate how available filter-design tools can be used to effectively design systems of varying complexity.

2 System Transformations

In the process of deriving the system and its analytical model, several system transformations will be used. This section offers a brief description of the important non-trivial transformations to be applied. Although presented in one direction, each is actually an equivalence which applies equally in both directions.

2.1 Sampling and digital filtering ↔ TDL filtering and sampling

The analysis of hybrid analog/digital systems is often complicated by the fact that the digital and analog filtering sections are separated by the sampler and its associated aliasing effects. Through this transformation, the digital filter following the sampler is moved back through the sampler, producing an analog tapped-delay-line (TDL) filter whose taps are spaced the same as the sampling rate and whose tap weights are just the coefficients of the digital filter. The cascade of the resulting periodic frequency response with preceding analog filters can then be readily seen.

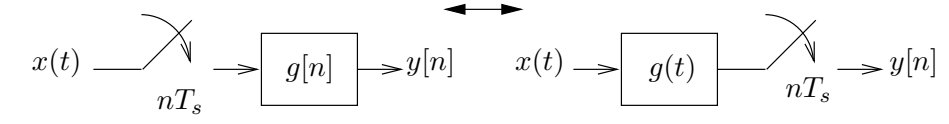

Trans. 1: Discrete-time filtering is moved before the sampler, forming an analog tapped-delay-line (TDL) filter.

The impulse response of the TDL filter is $g(t) = \sum_k g[k]\delta(t - kT_s)$, and its frequency response is $G(f) = \sum_k g[k]e^{-j2\pi kT_s f}$. The frequency response of the TDL filter is identical to that of its discrete-time counterpart except the former has an unnormalized frequency variable f, while the latter has a frequency variable normalized by sampling rate $1/T_s$. The equivalence between the two above systems can be shown by direct evaluation of their outputs. In the first, output $y[n]$ is the result of the discrete-time convolution of sequences $x(nT_s)$ and $g[n]$:

$$y[n] = \sum_k g[k]x((n-k)T_s). \tag{1}$$

In the second system, the output is samples of the continuous-time convolution of $x(t)$ and $g(t)$, $y[n] = (x \circledast g)(nT_s)$, which evaluates to (1).

2.2 Sampler followed by decimator

This simple transformation allows a sampler and a decimator to be combined into lower rate sampling.

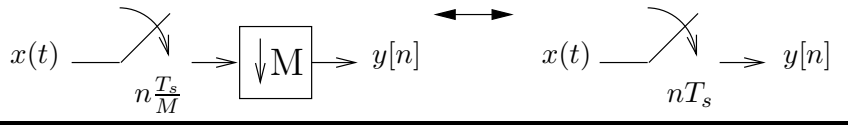

Trans. 2: Sampling and decimation combine to form lower-rate sampling.

2.3 Moving multipliers

Often it is desirable to move multipliers to one end of a system, so that the rest of the system becomes a baseband or passband equivalent. Moving a continuous-time multiplier past a sampler makes it a discrete-time multiplier.

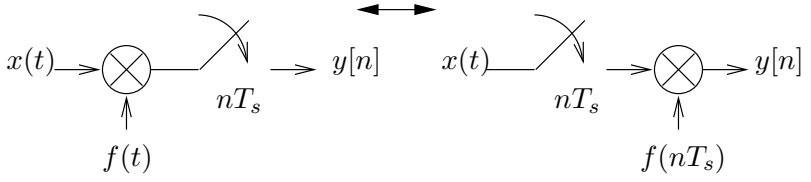

Trans. 3: Exchanging a multiplier and a sampler.

By defining the resulting multiplier input sequence in terms of the continuous-time function $f(t)$, the transformation is made reversible.

Moving a discrete-time multiplier past a decimator decimates the multiplier's input.

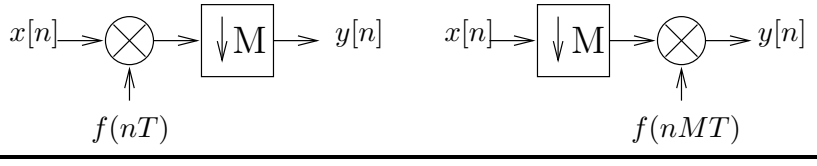

Trans. 4: Exchanging a multiplier and a decimator.

Again, defining the multiplier input sequence in terms of a continuous-time function $f(t)$ allows the transformation to be reversed.

Finally, a frequency shift (a multiplication by a complex exponential) can be moved past a filter by applying an opposite shift to the filter response.

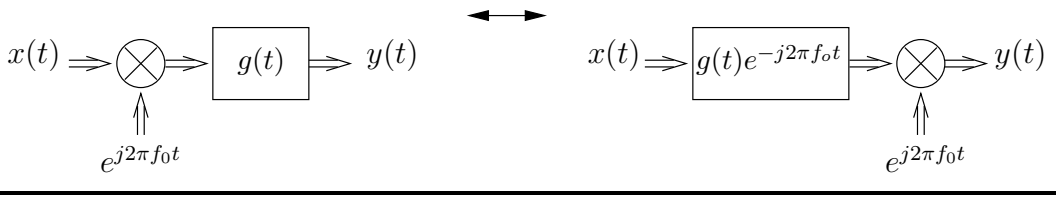

Trans. 5: Exchanging a frequency shift and a filter.

An identical relationship holds for discrete-time.

3 System Derivation

Using the transformations presented in Section 2, this section will derive a practical and simple IF-sampling demodulation architecture from the classic combination of analog demodulation and sampling. Along the way, an convenient equivalent system will be derived that simplifies analysis.

Figure 1(a) shows the classic quadrature demodulator, followed by I/Q sampling, digital fil-

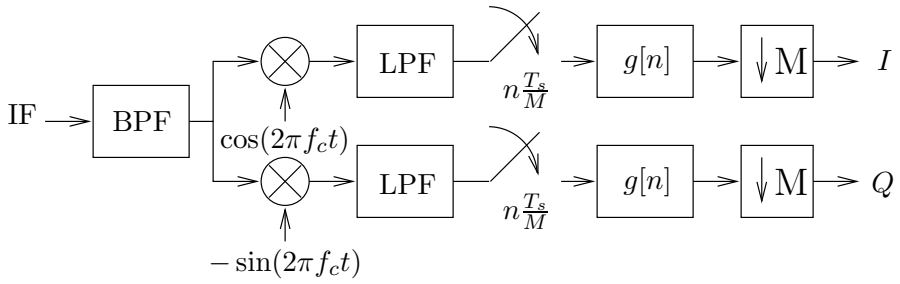

(a) Real signal representation.

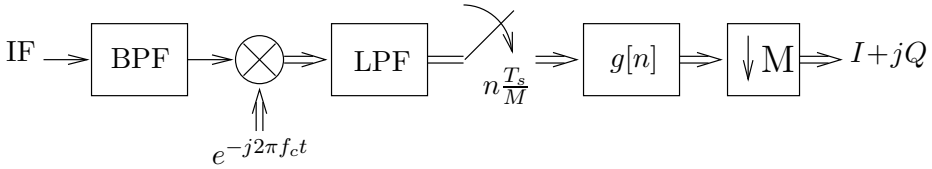

(b) Complex signal representation.

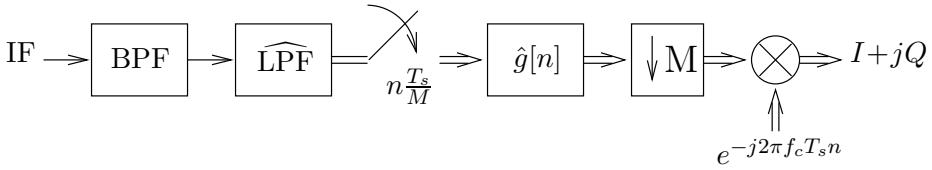

(c) Multiplication moved to discrete-time.

Figure 1: Real (a) and complex (b) signal representations of the classic analog demodulator with I-Q sampling and symbol-rate subsampling. Moving the multiplier right (c) makes it digital, but leaves behind the complex-impulse-response $\widehat{\text{LPF}}$. Double lines indicate complex quantities.

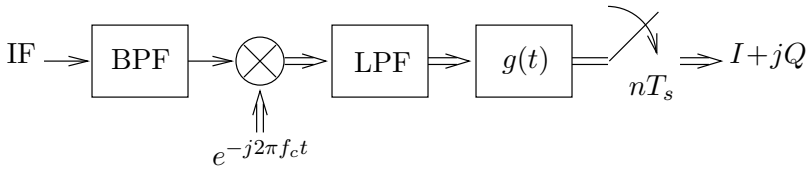

(a) Sampling and digital filtering are swapped, and the sampling and decimation combine.

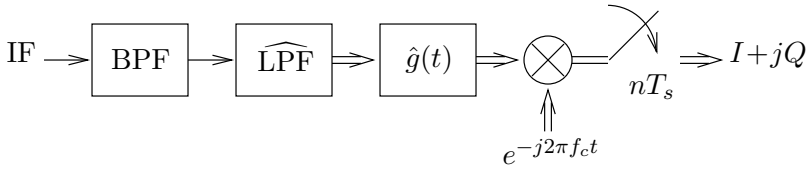

(b) The multiplier is moved past the filters.

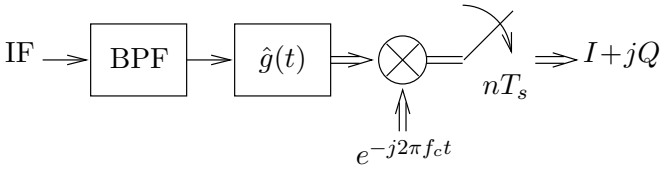

(c) With proper design of $\hat{g}(t)$, $\widehat{\text{LPF}}$ is no longer needed.

Figure 2: Transforming the analog demodulator to a system that requires no lowpass filter.

tering, and symbol-rate subsampling (decimation). Figure 1(b) is a convenient complex-signal representation of the quadrature demodulator. Since the performance of such a demodulator is often limited by the analog processing steps, a straightforward improvement is to move the multiplier to the right (using the transformations) past the LPF and the sampler so that a digital multiplier results. Optionally, it might be moved to the output, as in Fig. 1(c). The result is a new system in which both the lowpass filter LPF and the digital filter $g[n]$ have been shifted up in frequency. The impulse response $\text{LPF}(t)$ is replaced with response $\widehat{\text{LPF}}(t) = \text{LPF}(t)e^{j2\pi f_c t}$ and $g[n]$ is replaced with $\hat{g}[n] = g[n]e^{j2\pi n f_c T_s/M}$, resulting in complex impulse responses for both filters.

If not for the complex analog filter $\widehat{\text{LPF}}$, the system of Fig. 1(c) would be practical to implement. In fact, by rearranging the system in a manner more conducive to analysis, it can be shown that $\widehat{\text{LPF}}$ is not needed at all. A straightforward approach to the analysis of hybrid analog/digital systems of this sort is to transform them such that all the filter responses are in cascade. This allows the overall shaping and suppression requirements to be easily seen. The first step is to exchange the sampler and the digital filter $g[n]$, resulting in TDL filter $g(t)$ followed by the sampler. This sampler can then be combined with the decimator, resulting in the system of Fig. 2(a). The multiplier still separates the bandpass filter from the other two, so it is moved right past both the lowpass filter and the TDL filter in Fig. 2(b). Both filter responses are oppositely shifted as a result, and the new responses are labeled $\widehat{\text{LPF}}$ and $\hat{g}(t)$ as before.

Now that the three filters are in direct cascade, a spectral argument provides insight on the roles of the three filters. Figure 3 shows a set of example spectra for the system of Fig. 2(b). The IF signal shown has a root-raised-cosine shape with 50% excess bandwidth. The dotted signals represent adjacent channels. The cascade of the three filters BPF, $\widehat{\text{LPF}}$, and $\widehat{G}(f)$ must pass and shape only the desired positive-frequency lobe of the IF signal. As can be seen from the plots, $\widehat{\text{LPF}}$ is not needed if a stopband of $\widehat{G}(f)$ is placed in the same spectral region as the negative-frequency

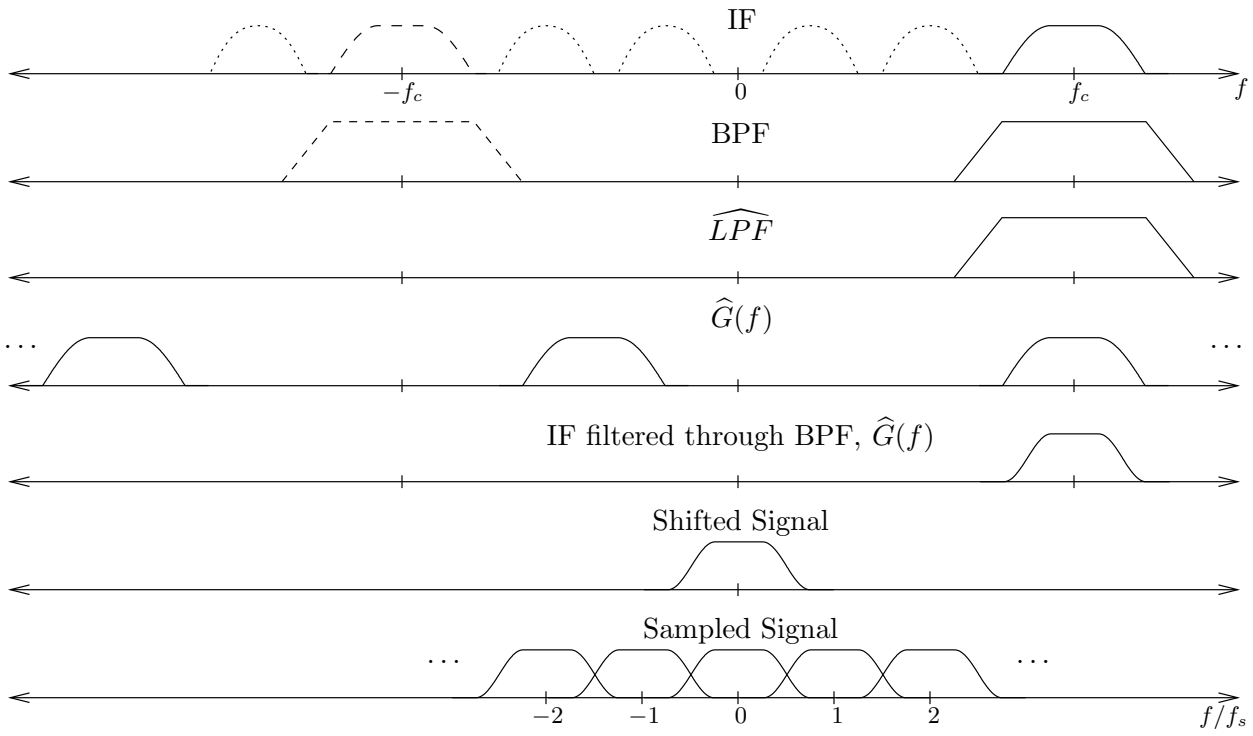

Figure 3: Example spectra that describe Figs. 2(b) and 2(c). Dashed lines indicate conjugation. Dotted lines represent adjacent channels.

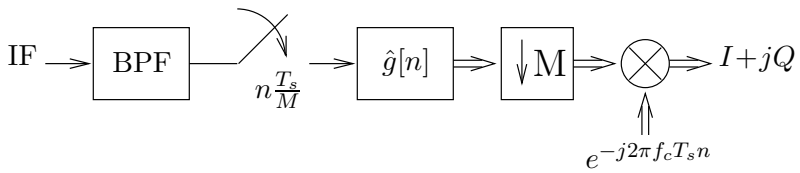

Figure 4: Final IF-sampling demodulator architecture.

portion of the BPF (and the IF signal). This can be done if there is enough available spectral control remaining after placing a passband in $\widehat{G}(f)$ to shape the desired positive-frequency portion of the IF signal. The response $\widehat{G}(f)$ is periodic with a period that is M times greater than the symbol rate (corresponding to the input sampling rate), so increasing M (the example uses $M = 5$) allows control over a larger bandwidth. However, the period of $\widehat{G}(f)$ must also be chosen such that none of the periodic replicas of its passband overlap the stopband region, or the two regions will conflict regardless of the total available design bandwidth. An important result is that the rate at which the IF signal is sampled (the input sampling rate Mf_s) is dependent on the bandwidth of the complex envelope and thus is not required to be twice the highest frequency of the IF, as in a conventional sampling system. The filter $\widehat{\text{LPF}}$ has been removed from the system of Fig. 2(c), which is a convenient system for design.

Having shown that proper design of $\hat{g}[n]$ (indirectly through design of $\hat{g}(t)$) eliminates the need for filter $\widehat{\text{LPF}}$, said filter can be removed from Fig. 1(c). Figure 4 shows the final demodulator system, which is exactly equivalent to Fig. 2(c). This system directly samples the output of a bandpass filter (possibly the equivalent response of previous stages) and performs digital filtering,

decimation, and frequency shifting. The filtering and decimation can be efficiently implemented by only calculating the samples to be kept, or through the use of a polyphase filter bank [20].

4 Design Examples

This section explores some simple approaches to choosing the system parameters and designing the digital filter $g[n]$. Since the system of Fig. 2(c) is more amenable to direct design, the digital filter will be designed indirectly through design of the TDL filter $g(t)$. The first example shows how simple design tools such as the Parks-McClellan algorithm [21] can be used to design the demodulator filter. A second example will present a more sophisticated linear programming approach.

4.1 A General Approach

A simplifying assumption that will be used in this paper is that the bandpass filter has done its job perfectly, and that only the desired real bandpass signal appears at the sampler input. This bandpass signal can be written as $P(f-f_c)+P^*(-f-f_c)$, a shifted version of the desired complex envelope response $P(f)$ and its conjugate reflection. The desired output of the filter response $G(f)$ is $P(f-f_c)D(f)$, the shifted envelope times some ideal desired function $D(f)$ that is often the match to the transmitted pulse. One simple approach would be to design $G(f)$ with as deep a stopband as possible in the region occupied by the conjugate reflection $P^*(-f-f_c)$ while approximating $D(f)$ as closely as possible (perhaps in an equiripple sense) in the region occupied by $P(f-f_c)$. This intuitive approach allows the designer to choose the relative importance of performance in the passband and stopband regions.

A somewhat more sophisticated approach would be to minimize the difference between the actual filter output and the ideal output. This error term is

$$P(f-f_c)[D(f)-G(f)]-P^*(-f-f_c)G(f), \tag{2}$$

with the first term representing error in the passband and the second term representing error in the stopband. This error might be minimized in the L_1, L_2, L_∞ or other sense as suggested by the application (or dictated by the design tools). Minimizing the L_2 norm (energy) of the error is a natural approach that requires quadratic optimization An L_1 norm, which places greater emphasis on regions of lesser magnitude than does an L_2, can be efficiently minimized using linear programming. Linear programming or the Parks-McClellan algorithm can be used to minimize the L_∞ norm of the error, producing an equiripple error term.

4.2 Design Using Parks-McClellan

In this example, a 1 MHz symbol rate signal with 35% excess-bandwidth root-raised-cosine pulse shaping is to be demodulated from an IF carrier frequency of 2.25 MHz. Filter response $G(f)$ must therefore be designed to matched-filter the incoming signal over a 1.35 MHz band centered at 2.25 MHz, while suppressing an equal interval centered around -2.25 MHz. The total independent response specification is therefore 2.7 MHz, so a filter response period (input sampling rate) of at least three times the symbol rate is needed for adequate spectral control. If the period is chosen to be 3 MHz then (by design) the carrier frequency is such that after placing a passband there the stopband region is symmetrically located between two successive copies of the passband, allowing

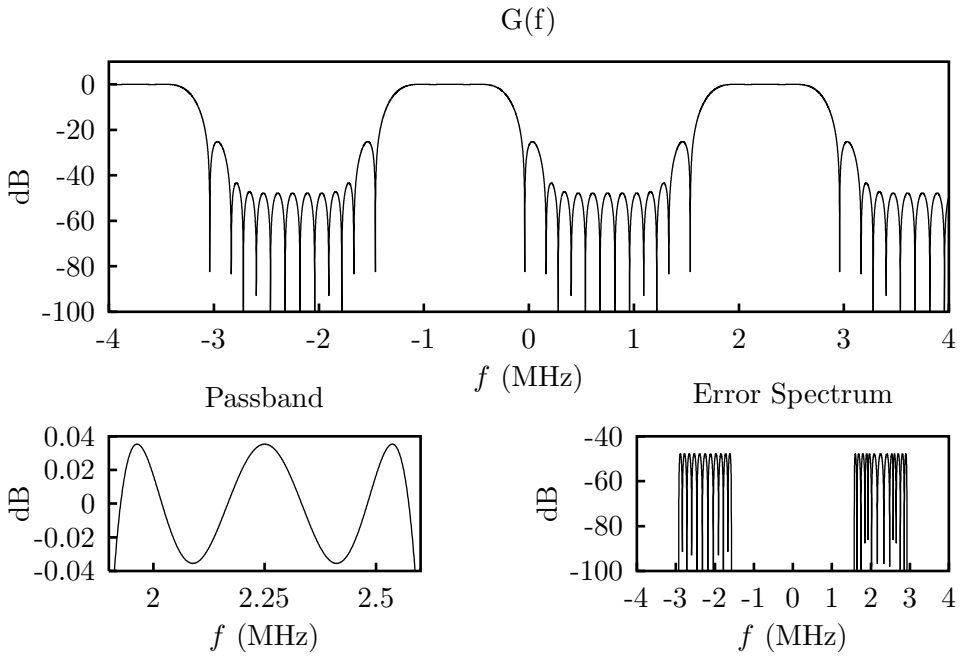

Figure 5: Filter frequency response, passband ripple, and error spectrum for Parks-McClellan design example.

independent specification of the stopband while leaving small transition bands. This symmetry, and the fact that the desired root-raised-cosine response is real and symmetric about frequency f_c, allows the use of the Parks-McClellan algorithm to design a real, linear phase baseband demodulation filter that can then be shifted to the passband.

The Parks-McClellan algorithm allows the design of real coefficient, linear phase FIR filters that are optimal in an equiripple sense. Specifically, the algorithm minimizes the maximum weighted error between the filter response and some desired function. Mathematically, the algorithm finds $\{G(f) : \min\{\max\{W(f)[D(f) - G(f)]\}\}\}$, where $W(f)$ is some real-valued weighting function, $D(f)$ is a real-valued desired response, and $G(f)$ is the response of the filter under design. If $W(f)$ is defined to be the incoming pulse $P(f - f_c) + P^*(-f - f_c)$, then this represents the L_∞ minimization of (2).

The usual implementations of Parks-McClellan only allow specification of $D(f)$ and $W(f)$, and therefore $G(f)$, on the normalized interval $[0, 0.5]$, since the filter period and symmetry then define the response everywhere. Since the design calls for a filter that is specified on disjoint intervals outside $[0, 0.5]$ and that is symmetric about f_c and not 0, modified versions of the desired function and weighting function are needed. A straightforward way to obtain $D(f)$ and $W(f)$ on the proper interval is to periodically extend the desired response ($P(f - f_c)$, a root-raised-cosine centered at f_c) and the weighting function ($P(f - f_c) + P^*(-f - f_c)$, two root-raised-cosines centered at f_c and $-f_c$) by the period of filter $G(f)$ (3 MHz), and then to shift both functions left by f_c. The interval $[0, 1.5\,\text{MHz}]$ of the resulting functions then represents the $D(f)$ and $W(f)$ needed by the optimization routine. After the filter is designed it can be shifted to its passband location by multiplying the taps by $e^{j2\pi n f_c/3\,\text{MHz}}$.

A 23-tap linear phase FIR filter was designed using the presented approach. Figure 5 shows the resulting response $G(f)$, the ripple in the flat portion of the passband, and the error term of (2).

This third plot shows that the error response is indeed equiripple.

4.3 Design Using Linear Programming

A more powerful design tool than Parks-McClellan for FIR filter design is linear programming. A linear program can minimize or maximize any function that is linear in the optimization variables (filter taps) subject to any (non-conflicting) linear constraints. The FF linear-programming language [22] will be used here to redo the design of the previous section, but with a different approach to minimizing the error term of (2). Additionally, the filter will be designed to null any DC errors from the A/D converter.

The code for the FF program will be presented, with discussion, in several parts. This first portion defines some constants to be used later in the program.

Let $s = 1$, let $c = 2$, and let MHz $= 1$.
Index T from 1 to 2, let $T_s = \frac{1}{1\,\text{MHz}}$, and let $T_c = \frac{1}{2.25\,\text{MHz}}$.
Let $M = 3$, and let $N = 12$.

The filter to be designed will again be a 23-tap linear-phase filter, but now the coefficients can be complex.

Index g from 0 to $N-1$, and let (g, G) be a Fourier transform pair.
Let g_0 be an optimized, real tap at 0 delay, and
let $g_1, \ldots, g_{N-1}$ be optimized, complex tap pairs at $\pm\frac{T_s}{M}, \ldots, \pm(N-1)\frac{T_s}{M}$ delay.

This code defines the TDL filter structure in terms of an array of optimization variables. The taps here are given symmetric spacing about $t = 0$ for convenience. Function $G(f)$ is defined to be the response of the filter.

Interpolate P from real file "RRC.dat" with spacing $\frac{M}{4000T_s}$ from $-\frac{M}{4T_s}$.
Let $\alpha = 0.35$.

This code defines the function $P(f)$ by linearly interpolating between values read from a datafile. These data values were calculated elsewhere as a root-raised cosine with an excess bandwidth of α.

The approach that will be taken will be to minimize the L_1 norm of the error term given in (2). Choosing the desired response $D(f)$ to be the match to the transmitted pulse $P(f - f_c)$, the function to be minimized is

$$\int \big|P(f-f_c)[P^*(f-f_c) - G(f)] - P^*(-f-f_c)G(f)\big|df.$$

The function $P(f)$ is real, so $P(f) = P^*(f)$. Since the integrand is nonzero only over two disjoint, finite regions (namely the intervals $\pm[f_c - \frac{1+\alpha}{2T_s}, f_c + \frac{1+\alpha}{2T_s}]$, where α is the excess bandwidth of $P(f)$) the integral can be approximated by two summations over appropriate grids of frequencies. Minimizing the sum

$$\sum_k \big|P(f_k^+ - f_c)[P^*(f_k^+ - f_c) - G(f_k^+)]\big| + \sum_k \big|P^*(-f_k^- - f_c)G(f_k^-)\big|, \tag{3}$$

where the frequencies f_k^+ are on a grid covering the passband, and the frequencies f_k^- cover the stopband region, approximately minimizes the integral. This sum is not itself linear in the filter

taps, but it can be minimized using two sets of non-negative auxiliary optimization variables β and γ. Enforcing the linear constraints

$$-\beta_k \le P(f_k^+ - f_c)[P^*(f_k^+ - f_c) - G(f_k^+)] \le \beta_k$$
$$-\gamma_k \le P^*(-f_k^- - f_c)G(f_k^-) \le \gamma_k$$

allows minimization of the sum of the auxiliary variables to minimize (3).

Let $L = 45$, index β from $-L$ to L, index γ from $-L$ to L,
let $\beta_{-L}, \ldots, \beta_L$ be optimized and bounded below by 0, and
let $\gamma_{-L}, \ldots, \gamma_L$ be optimized and bounded below by 0.

This code declares the auxiliary optimization variables β and γ. The parameter L controls the resolution of the frequency grid over which the summations are performed. The choice of L was determined experimentally. A smaller value would introduce errors in the integral approximation, while a larger value would just force more computation.

Require $G(0) = 0$.
For each $k = -L, \ldots, L$, let $f = T_c^{-1} + \frac{k}{L}\left(\frac{1+\alpha}{2T_s}\right)$, and
    require $|P(f - T_c^{-1})[P(f - T_c^{-1}) - G(f)]| \le \beta_k$.
For each $k = -L, \ldots, L$, let $f = -T_c^{-1} + \frac{k}{L}\left(\frac{1+\alpha}{2T_s}\right)$, and
    require $|P(-f - T_c^{-1})G(f)| \le \gamma_k$.

Minimize $\sum_{k=-L}^{L}(\beta_k + \gamma_k)$, and
write "L1 error=",$\frac{1+\alpha}{2(2L+1)T_s}\sum_{k=-L}^{L}(\beta_k + \gamma_k)$ to report.

For each $n = N-1, \ldots, 1$, write $\Re(g_n)$," ",$-\Im(g_n)$ to output.
For each $n = 0, \ldots, N-1$, write $\Re(g_n)$," ",$\Im(g_n)$ to output.

This final code fragment performs the minimization just discussed. The first constraint places a null in $G(f)$ at DC. Since the filter being designed immediately follows the sampler, a null in the DC response of the filter will serve to cancel any A/D DC errors. This constraint does, however, use up a degree of freedom, and it causes the filter response to be asymmetric (although a second null could be placed to maintain the symmetry). The next four lines define the frequency grid and set the constraints on the optimization variables β and γ. The "Minimize" line tells the interpreter to perform the optimization, minimizing the sum of the auxiliary optimization variables (and in so doing, the L_1 norm of the error). Finally, the value of the L_1 norm and the optimized filter taps are written out. Figure 6 shows the resulting filter response, passband ripple, and error spectrum.

Comparing these results to those using Parks-McClellan shows that the L_1-minimized filter has greater suppression over most of the stopband, and less ripple over most of the passband. These gains were achieved with a modest loss in performance near the transition bands. The second filter does not drop off as rapidly as the first, which shows up as peaks the error term near the transitions. The error terms show that, although the error in the second filter is less than the error in the first for almost all frequencies, it does peak up higher briefly in the passband. Thus both filters are optimum in the sense in which they were designed, and the application would dictate which (if either) is more suitable.

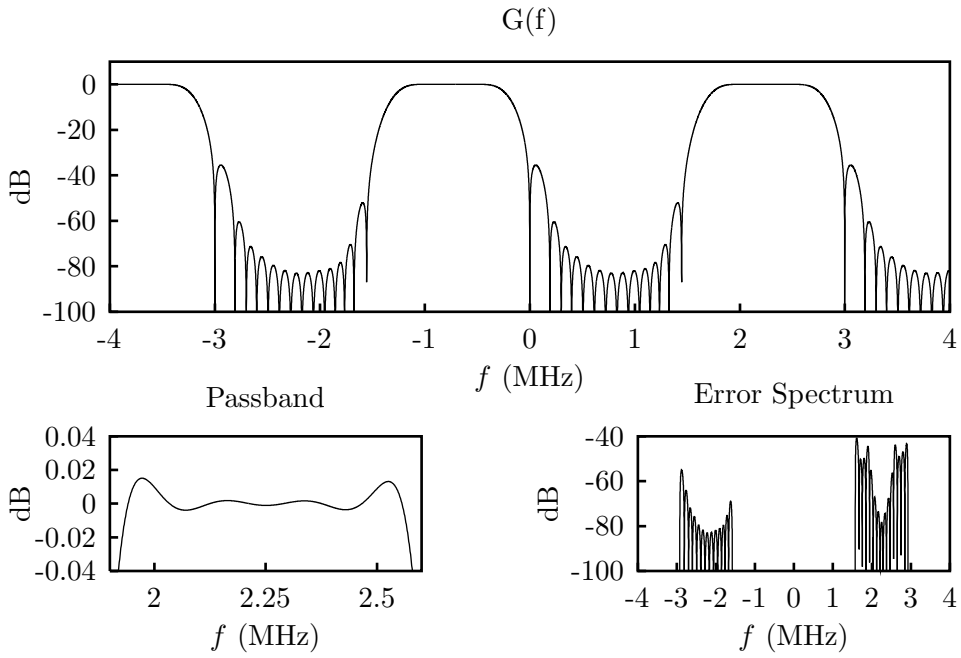

Figure 6: Filter frequency response, passband ripple, and error spectrum for linear-programming design example.

4.4 Other Design Approaches

The examples presented here are much simplified, and as such only scratch the surface of available design tools and methods. One drawback of this error-minimization design approach is that it is not immediately clear how the "error" term relates to system performance metrics such as bit-error-rate or intersymbol interference. When such measures are of interest, the more sophisticated linear-programming techniques found in [22] can be easily adapted to the current system. It is rare for a system to contain only a single, isolated filter, and so the cascade response of all the filtering steps may be more important than the single digital filter response designed in the examples. Examples of the direct design of analog-digital cascade responses can also be found in [22]. Certainly other tools than Parks-McClellan and linear programming exist for the design of FIR filters: the eigenfilter method [23] and semidefinite programming [24] are examples of techniques that allow quadratic optimization.

References

[1] A. Kohlenberg, "Exact interpolation of band-limited functions," *J. Appl. Phys.*, vol. 24, no. 12, Dec. 1953.

[2] D. A. Linden, "A discussion of sampling theorems," *Proceedings of the IRE*, vol. 47, no. 7, pp. 1219–1226, July 1959.

[3] Alan J. Coulson, "A generalization of nonuniform bandpass sampling," *IEEE Trans. on Signal Processing*, vol. 43, no. 3, pp. 694–704, Mar. 1995.

[4] W. M. Waters and B. R. Jarrett, "Bandpass signal sampling and coherent detection," *IEEE Trans. Aerosp. Electron. Syst.*, vol. AES-18, no. 4, pp. 731–6, Nov. 1982.

[5] D. W. Rice and K. H. Wu, "Quadrature sampling with high dynamic range," *IEEE Trans. Aerosp. Electron. Syst.*, vol. AES-18, no. 4, pp. 736–9, Nov. 1982.

[6] W. Rosenkranz, "Quadrature sampling of FM-bandpass signals–implementation and error analysis," in *Digital Signal Processing — 87. Proceedings of the International Conference*, 1987, pp. 377–81.

[7] J. B. Mariño and E. Masgrau, "Sampling in-phase and quadrature components of band-pass signals," *Signal Processing*, vol. 20, no. 2, pp. 121–5, June 1990.

[8] James P. Hansen, "Ultra high performance direct sampling quadrature detectors," Tech. Rep., Naval Research Laboratory, Radar Division, Apr. 1991, Unpublished.

[9] E. Hermanowicz, "Practical digital complex sampling scheme," *Electron. Lett.*, vol. 27, no. 5, pp. 460–2, Feb. 1991.

[10] Leopold E. Pellon, "A double nyquist digital product detector for quadrature sampling," *IEEE Trans. on Signal Processing*, vol. 40, no. 7, pp. 1670–1680, July 1992.

[11] F. Oscarsson and A. Lindblad, "Wideband HF receiver with digital quadrature splitting," in *Proc. of the Fourth International Conf. on Signal Proc. Applications and Tech.*, 1993, vol. 2, pp. 1267–71.

[12] A. K. Halberstadt, "Application of frequency-domain polyphase filtering to quadrature sampling," *Proceedings of the SPIE*, vol. 2563, pp. 450–7, 10-12 July 1995.

[13] Charles M. Rader, "A simple method for sampling in-phase and quadrature components," *IEEE Trans. Aerosp. Electron. Syst.*, vol. AES-20, no. 6, pp. 821–824, Nov. 1984.

[14] R. L. Mitchell, "Creating complex signal samples from a band-limited real signal," *IEEE Trans. Aerosp. Electron. Syst.*, vol. 25, no. 3, pp. 425–427, May 1989.

[15] H. R. Ward, "An optimum filter for direct A/D conversion," *IEEE Trans. Aerosp. Electron. Syst.*, vol. 27, no. 6, pp. 883–886, Nov. 1991.

[16] X. Chen, J. H. Lodge, K. E. Scott, and A. M Sendyk, "Quadrature splitter considerations for digital cellular radio," in *Conference Record of The Twenty-Sixth Asilomar Conference on Signals, Systems and Computers*, 1992, vol. 2, pp. 606–11.

[17] T. Wada, S. Takeya, M. Shinonaga, and H. Miyauchi, "Developement of I/Q sampling technology (radar applications)," *IEICE Trans. on Comm.*, vol. E77-B, no. 2, pp. 270–2, Feb. 1994.

[18] Henry Samueli and Bennett C. Wong, "A VLSI architecture for a high-speed all-digital quadrature modulator and demodulator for digital radio applications," *IEEE J. Select. Areas in Commun.*, vol. 8, no. 8, pp. 1512–1519, Oct. 1990.

[19] S. C. Pohlig, "Digital signal processing for space-based radar," Proj. Rep. SRT-30, MIT Lincoln Laboratory, Sept. 1988.

[20] P. P. Vaidyanathan, "Multirate digital filters, filter banks, polyphase networks, and applications: A tutorial," *Proc. of the IEEE*, vol. 78, no. 1, Jan. 1990.

[21] James H. McClellan, Thomas W. Parks, and L. R. Rabiner, "A computer program for designing optimum FIR linear phase digital filters," *IEEE Trans. on Audio and Electroacoustics*, vol. AU-21, no. 6, Dec. 1973.

[22] Jeffrey O. Coleman, *The Use of the FF Design Language for the Linear-Programming Design of Finite-Impulse-Response Digital Filters for Digital-Communication and Other Applications*, Ph.D. thesis, University of Washington, Seattle, WA, Dec. 1991.

[23] P. P. Vaidyanathan and T. Q. Nguyen, "Eigenfilters: A new approach to least-squares FIR filter design and applications including nyquist filters," *IEEE Trans. Circuits Syst.*, vol. CAS-34, no. 1, Jan. 1987.

[24] Rajesh R. Venkatraman and Jeffrey O. Coleman, "A test-waveform view of the quadratic design of fir filters," in *Proc. ICSPAT '96, The 7th Int'l Conf. on Signal Proc. Applications and Tech.*, Oct. 1996.